Investigation of the structure of thin HfO_2 films by soft x-ray reflectometry techniques

2009 J. Phys.: Condens. Matter 21 185012

(http://iopscience.iop.org/0953-8984/21/18/185012)

J. Phys.: Condens. Matter **21** (2009) 185012 (7pp) doi:10.1088/0953-8984/21/18/185012

Investigation of the structure of thin HfO_2 films by soft x-ray reflectometry techniques

E O Filatova[1], A A Sokolov[1], I V Kozhevnikov[2], E Yu Taracheva[1], O S Grunsky[3], F Schaefers[4] and W Braun[4]

[1] St Petersburg State University, Institute of Physics, St Petersburg, 198504, Russia
[2] Institute of Crystallography, Moscow, 119333, Russia
[3] St Petersburg State University, Geological Faculty, St Petersburg, 198504, Russia
[4] BESSY, Albert Einstein Straße 15, D-12489 Berlin, Germany

E-mail: feo@EF14131.spb.edu

Received 19 September 2008, in final form 5 March 2009
Published 31 March 2009
Online at stacks.iop.org/JPhysCM/21/185012

Abstract

HfO_2 thin films of different thicknesses and deposited by two methods (ALD and MOCVD) were studied. The microstructure of films was characterized by reflection spectroscopy, x-ray diffraction (XRD), and soft x-ray reflectometry. It was established that the HfO_2 film microstructure is closely dependent on film thickness. The 5 nm thick film synthesized by ALD shows an amorphous phase while the film prepared by MOCVD was inhomogeneous in depth and showed signs of crystalline structure. First results on the reconstruction of the depth distribution of chemical elements based on the analysis of reflectivity curves are discussed.

(Some figures in this article are in colour only in the electronic version)

1. Introduction

HfO_2 is one of the most promising materials for the nanoelectronics industry to replace SiO_2 because it has a high dielectric constant [1, 2] and is expected to be stable in contact with Si. So far one stable monoclinic phase and four metastable phases, cubic, tetragonal, orthorhombic I and orthorhombic II, have been identified for HfO_2 [3]. An amorphous modification can also be fabricated [4]. Although the tetragonal HfO_2 structure has the highest dielectric permittivity [3] an amorphous structure is to be preferred for several reasons. First of all amorphous materials do not contain grain boundaries or dislocations that can trap charge and offer fast diffusion pathways for leakage current. In addition, stresses in amorphous materials can be taken up by small variations in the random network, where they may likewise be taken up by misfit dislocations in a polycrystalline material. Amorphous structures also tend to minimize electronically active defects, but may give rise to shallow traps. Epitaxial films can be produced free of grain boundaries and defects and, therefore, are usually preferred for gate dielectrics. Therefore, most of the work on HfO_2 has been focused on manufacturing amorphous films to replace SiO_2, but this process is unpredictable, because the microstructure of films is largely dependent on thickness, technology of synthesis and utilizable precursors [5–7]. It is known that thin films of less than 10 nm thickness usually have an amorphous structure. At the same time there is work [5] where films of thickness 4 and 6 nm already exhibit the sign of crystalline structure. Crystalline films often have monoclinic structure [5], but can also have mixed monoclinic and tetragonal [7]. Therefore the technology of preparing films, i.e. method and condition of synthesis (rate of deposition, temperature of substrate, etc), also as utilizable precursors is an important issue to fabricate films with the required properties. A further study of the effect of different factors is required. In this paper we focus on the discussion of crystalline and electronic structure of thin films of HfO_2 of different thicknesses and prepared by two methods (atomic layer deposition (ALD) and metal organic chemical vapor deposition (MOCVD)). First results on the reconstruction of the dielectric function profile of HfO_2 films on the basis of reflectivity curves are discussed.

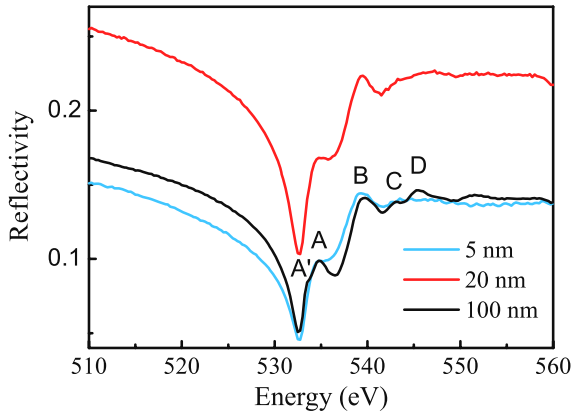

Figure 1. O 1s reflection spectra of HfO_2 5, 20 and 100 nm thick films synthesized by ALD and measured at a grazing incidence angle of 4°.

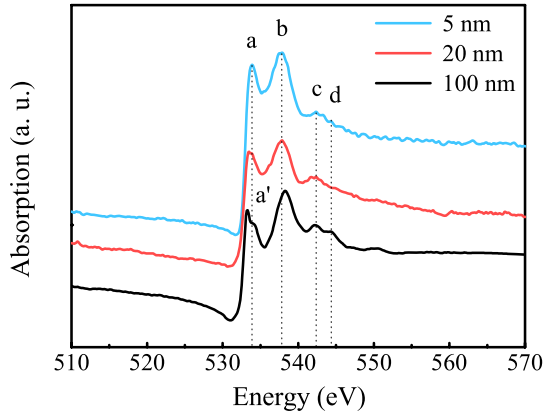

Figure 2. Absorption spectra calculated on the bases of the measured reflection spectra (figure 1) using a Kramers–Kronig analysis.

2. Experiment

HfO_2 films were synthesized by ALD and MOCVD methods. The films were deposited on (100) n-type silicon wafers by ALD, using hafnium tetrachloride ($HfCl_4$) and water at 300 °C substrate temperature. Different film thicknesses (5, 20 and 100 nm) were obtained by varying the number of ALD cycles only.

When the MOCVD method was used, HfO_2 films were deposited on (100) n-type silicon wafers using tetrakisdiethylaminohafnium ($Hf(N(C_2H_5)_2)_4$) and O_2 at 485 °C substrate temperature.

The angular and spectral dependences of reflectivity in the vicinity of the O K(1s) absorption edge were measured using s-polarized synchrotron radiation in the reflectometer set-up on the optics beamline (D-08-1B2) at the BESSY-II synchrotron radiation facility of the HZB, Germany. All spectra were measured with an energy resolution better than 0.3 eV. The accuracy of the energy scale was 0.1 eV. The angular dependences of the reflectivity were measured with an angular resolution better than 0.001°. A GaAsP diode together with a Keithley electrometer 617 was used as detector. The entrance aperture of the detector was 4 mm^2. Monitoring of the changes in the incidence beam was carried out with the help of Au mesh.

The XRD measurements were carried out on a Rigaku Miniflex II benchtop x-ray diffractometer with Bragg–Brentano geometry and Cu $K\alpha_1\alpha_2$ (0.154 178 nm) radiation. The angular resolution was better than 0.02°.

3. Results and discussion

3.1. HfO_2 films of different thicknesses synthesized by ALD

The O 1s reflection spectra of HfO_2 films 5, 20 and 100 nm thick synthesized by ALD and measured at a grazing incidence angle of 4° are presented in figure 1. It can be seen that the reflection spectra of different film thicknesses are similar in the number of essential features and their energy positions. At the same time, there is an additional detail (shoulder A') in the spectrum of the thick film (100 nm). The reflection spectra of the 5 and 100 nm thick films correlate rather well in the absolute value of reflectivity, but the reflectivity for these films is far below the reflectivity of the 20 nm thick film.

To analyze the observed differences the absorption spectra were calculated on the basis of the measured reflection spectra by means of the Kramers–Kronig transform (KKT) using the method described in detail in [8]. We recall briefly here the KKT method: from the absolute reflectivity $R(E, \theta)$ where E is the energy of the radiation and θ is the glancing incident angle, it is possible to calculate the phase shift $\psi(E_0)$ of the reflection amplitude $r = \rho \exp(i\psi)$ with $R = \rho^2$, according to the formula

$$\psi(E_0) = \frac{E_0}{\pi} \mathrm{PV} \int_0^\infty \frac{\ln R(E, \theta)}{E^2 - E_0^2} \mathrm{d}E \qquad (1)$$

where PV stands for the principal value. Using the Fresnel relationship, one deduces the absorption coefficient. Let us emphasize that, in principle, the domain of integration extends over the entire spectral domain (i.e. E runs from zero to infinity). Of course, in practice, the domain of integration is restricted to a finite region covering the domain of measurement and extensions outside this domain where semi-empirical formulae are used for $R(E)$. In the present study, it has been assumed that the integration domain is large enough not to affect the physical results. The calculated absorption spectra are presented in figure 2.

To understand the dynamics of the formation of the O 1s absorption spectrum of HfO_2 it is necessary to remember that according to calculations of the partial DOS the lower conduction band of HfO_2 is formed solely by 3d states of Hf [3], which are sensitive to the violation of local symmetry and a decrease of the coordination number. Due to the effect of the crystal field from the oxygen atoms on the Hf d states, the fivefold degenerated 2D term of the free ion is split into two components in the ligand field: doubly degenerated 2E (e_g) and triply degenerated 2T2 (t_{2g}) components. The molecular orbitals of HfO_2 derived from a linear combination of atomic orbitals (LCAO) are characterized by four unoccupied orbitals [5]:

e_g(Hf 5d + O 2pπ), t_{2g}(Hf 5d + O 2pσ), a_{1g}(Hf 6s + O 2p) and t_{1u}(Hf 6p + O 2p). In this classification one can expect four features in the O K absorption spectrum of HfO_2 connected with one electron transitions from the O 1s orbital to the empty electronic states e_g, t_{2g}, a_{1g} and t_{1u}.

The analysis of the energy position of the peaks in the absorption spectra of the films of different thicknesses (figure 2) shows that the energy separation between peaks a and b is equal to 3.7 eV (film of 5 nm thickness), 4.3 eV (film of 20 nm thickness) and 5.1 eV (film of 100 nm thickness) within the experimental accuracy, that is close to the splitting of Hf 5d states into t_{2g} and e_g components in the anisotropic field of the tetrahedral oxygen. The values obtained agree well with the experimental value of the effective crystal-field splitting of HfO_2, that is equal to 4.3 eV [9, 10]. Peaks a and b therefore reflect core-electron transitions in the oxygen atoms to the lowest unoccupied Hf de_g and Hf dt_{2g} electronic states, that are hybridized with the 2p states of the oxygen atoms.

Let us look at feature a (doubly degenerated e_g component) (figure 2). Obviously, there is a broadening of this feature with the growth of the film thickness. Moreover feature a demonstrates a double structure a–a′ in the absorption spectrum of the film of 100 nm thickness. It is known that the state degeneracy can be removed due to local symmetry distortions or a decrease in coordination number. An analysis of different phases of HfO_2 allows us to establish the following facts.

For a cubic HfO_2 structure, each metal ion is surrounded by eight equivalent O atoms (eight-coordinated environment of the Hf ion) and there is a four-coordinated environment of the O atom. The tetragonal HfO_2 structure has the metal ions in a distorted eightfold coordination that can only lead to a slight broadening of peaks a and b. But the monoclinic phase has sevenfold coordinated metal ions (sd^3p^3 hybridization), that leads to a splitting of the e_g component caused by the dynamic Jahn–Teller effect [5]. Suppression of the Jahn–Teller d state degeneracy splitting takes place, according to [5], because of grain size effects when grain size $\lesssim$ 2 nm. Respectively, it might be concluded that the 100 nm thick film has the polycrystalline structure with size of the grains $\gtrsim$ 2 nm. Moreover, the microstructure of the thick film involves essentially the monoclinic phase.

Bands c and d in the O 1s spectrum of the 100 nm thick film have to be related to the empty electronic states with mixed (Hf 6s, 6p + O 2p) character. The probability of the transitions to these states is rather low. So, the double structure c–d cannot be observed in the amorphous state of the film. As can be seen from figure 2 there is only one wide band c in the spectra of 5 and 20 nm thick films. This result agrees well with experimental results [3, 5, 7] demonstrating the dependence of the manifestation of bands c and d, accompanied by a manifestation of Jahn–Teller effect, on the size of the grains. Even in the case of signatures of ordering on a subnanometer scale in the film one can see a slight splitting of the features c–d. The best resolution of this structure is accompanied by a manifestation of the Jahn–Teller effect [5].

One can conclude that, according to the reflection spectroscopy investigations, the 5 and 20 nm thick films

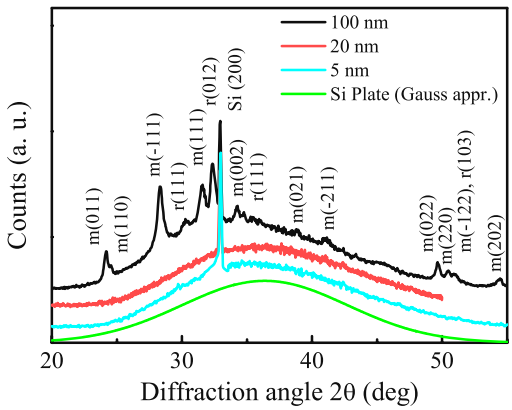

Figure 3. XRD data for HfO_2 5, 20 and 100 nm thick films synthesized by ALD. The letters *m* and *r* represent the monoclinic and orthorhombic structure of the HfO_2 film, respectively.

are amorphous, while the film of 100 nm thickness is polycrystalline essentially in the monoclinic phase.

According to the literature HfO_2 films of thickness lower than 10 nm are traditionally amorphous. In line with our investigations the 20 nm thick film is amorphous too.

The films mentioned above were characterized by XRD (figure 3) with the goal to study the structure and phase composition stability depending on the film thickness. XRD data for Si(100) substrates before film synthesis have been obtained to take into account the background. Using the Gauss's approximation of the radiograph of the Si(100) substrate the background has been constructed.

As can be seen from figure 3, the 100 nm thick film has a practically (100%) crystalline structure and consists of two phases (monoclinic and orthorhombic). The comparative analysis of the intensities of diffraction peaks of XRD data of the film under consideration and HfO_2 powder (data file *ICDD 43*–1017 and *ICDD 40*–1173, table 1) allows us to establish that there is no preferred orientation of crystallites of both phases in the film. The crystallite sizes were calculated using the Selyakov–Scherrer formula [11]:

$$L_{cr} = \frac{\lambda \cos\theta}{\sqrt{B_{2\theta}^2 - b^2}} \qquad (2)$$

where L_{cr} is the size of the grain, λ is the wavelength of the incident beam (0.154 178 HM), θ is the reflection angle, $B_{2\theta}$ is the halfwidth of the peak and b is the broadening caused by the diffractometer (the width of the Si(200) reflection peak was used as an etalon). Table 1 shows the results of the calculations. As can be seen from the table, sizes of the crystallites of different orientations are distinguished slightly.

According to XRD data, there is no crystalline phase in HfO_2 films of thicknesses 5 and 20 nm.

One can see that results obtained from reflection spectra correlate well with XRD data.

3.2. HfO_2 films synthesized by ALD and MOCVD

A similar analysis of the structure of films of equal thicknesses of 5 nm, but fabricated by two different methods (ALD and

Table 1. XRD data for HfO_2 100 nm thick.

No	2θ	Int (meas, a.u.)	Int (ICDD)	Phase (system)	S.G.	(hkl)	Peak halfwidth	L_{cr} (nm)
1	24.1532	515.8	15	HfO_2 (monoclinic)	$P21/c$	011	0.34	27.3
2	24.5185	160.3	12	HfO_2 (monoclinic)	$P21/c$	110	0.28	33.6
3	28.2733	1132.2	100	HfO_2 (monoclinic)	$P21/c$	$\bar{1}11$	0.58	15.8
4	30.2837	175.8	40	HfO_2 (orthorhombic)	$Pmnb$	101	0.5	18.5
5	31.5338	719.9	74	HfO_2 (monoclinic)	$P21/c$	111	0.52	17.9
6	32.3559	1092.4	100	HfO_2 (orthorhombic)	$Pmnb$	012	0.51	18.3
7	32.8969	2443.4	—	Si (cubic)		200	0.08	—
8	34.1835	282.2	25	HfO_2 (monoclinic)	$P21/c$	002	0.32	29.8
9	49.6343	351.3	16	HfO_2 (monoclinic)	$P21/c$	022	0.40	24.8
10	50.4033	183.1	18	HfO_2 (monoclinic)	$P21/c$	220	0.39	25.6
11	54.3407	130.6	11	HfO_2 (monoclinic)	$P21/c$	202	0.38	26.7

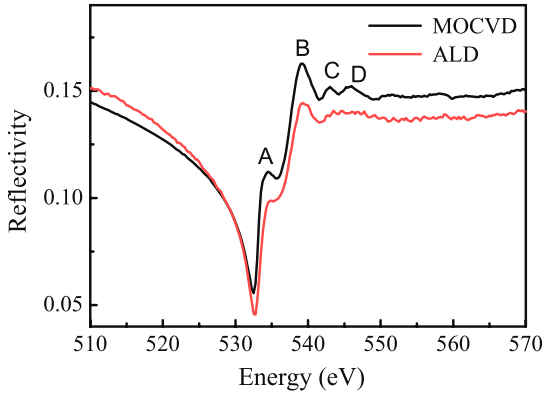

Figure 4. O 1s reflection spectra of films 5 nm thick fabricated by different methods (ALD and MOCVD) measured at a grazing incidence angle, 4°.

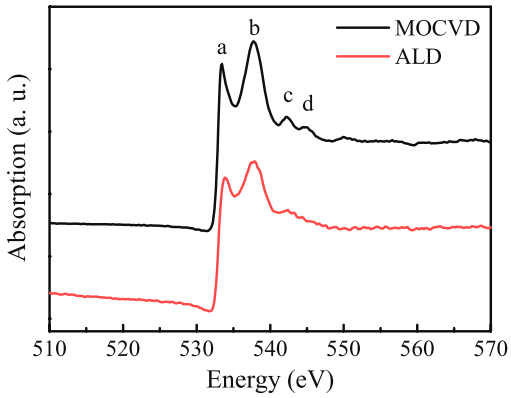

Figure 5. O 1s absorption spectra of 5 nm thick films fabricated by different methods (ALD and MOCVD) calculated from reflection spectra (figure 4).

MOCVD), was carried out. Figure 4 shows the O 1s reflection spectra of films measured at a grazing incidence angle, 4°. The O 1s absorption spectra calculated from reflection spectra (figure 4) using a Kramers–Kronig analysis are presented in figure 5.

Analysis of the shape of reflection and absorption spectra (figures 4, 5) shows good agreement between the spectra of films grown by two different methods. Obviously, bands c and d in the spectrum of the film synthesized by MOCVD are clearly distinguished. Taking into account the results obtained in part A it can be concluded that the film manufactured by ALD is amorphous, whereas the film prepared by the MOCVD method has signatures of ordering of the structure because of the pronounced details c and d. In contrast to the above-described case for the 100 nm thick film manufactured by ALD (figures 1 and 2) there is no sign of a Jahn–Teller splitting in the spectrum of the film prepared by MOCVD, that allows us to assume that grain size in the film under consideration is <2 nm. It can be argued that the film prepared by MOCVD shows evidence for crystallization.

In addition to reflection spectra, the reflectivities versus grazing angle were measured at different wavelengths of the incident beam for HfO_2 films under consideration. The reflectivities versus grazing angle measured at two different wavelengths of the incident beam are shown in figures 6 and 7, circles, respectively. Evidently, the reflectivity curve contains information about the depth distribution of the dielectric function. Moreover, measuring reflectivity curves at different wavelengths, one can try to deduce information about the depth distribution of chemical elements composing the sample studied. However, the inverse problem of x-ray reflectometry is well known to be ambiguous, and, as a rule, there is an infinite number of different dielectric function profiles resulting in the same reflectivity curve measured in a limited angular interval. A review of existing approaches to the solution of the inverse problem of x-ray reflectometry is presented, e.g., in [12, 13].

A novel approach to the inverse problem was developed in [14]. The key feature of this approach consists in modeling the reflectivity amplitude over the entire range of incidence angles, including the non-physical complex angles. Such a consideration has proved to allow the reconstruction of the dielectric constant distribution by simply using the general model for reflecting media: it is sufficient to know the points of discontinuity, where the dielectric function itself or its nth derivative undergoes a step-like variation. In turn, information about points of discontinuity can be extracted from the reflectivity curve measured experimentally. Notice that until now the approach was used only in the hard x-ray region, where absorption of radiation can be neglected at least for thin films.

One of the crucial points preventing a unique solution of the inverse problem is the absence of information about the

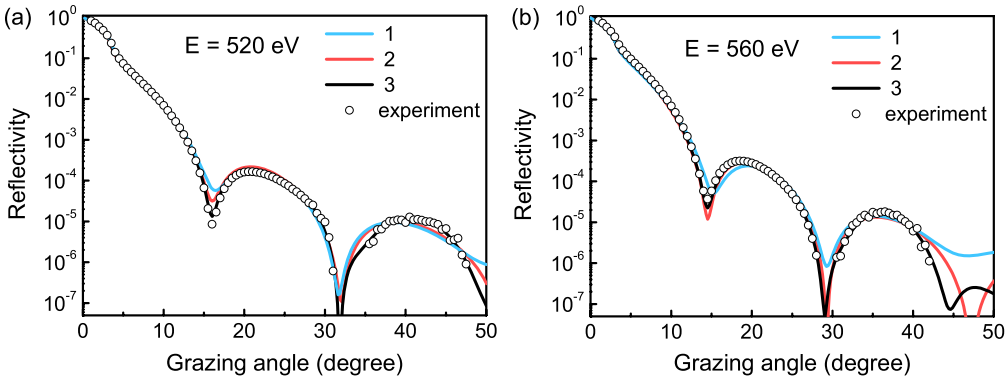

Figure 6. The measured reflectivity curves (circles) versus grazing angle at two energies ((a) 520 and (b) 560 eV) of the 5 nm thick HfO_2 film deposited onto a Si substrate by the ALD technique. Curves 1 and 2 are the result of fitting with the use of the single-layer (1) or three-layer (2) models. Curves 3 are the result of a numerical refinement of the tri-layer model.

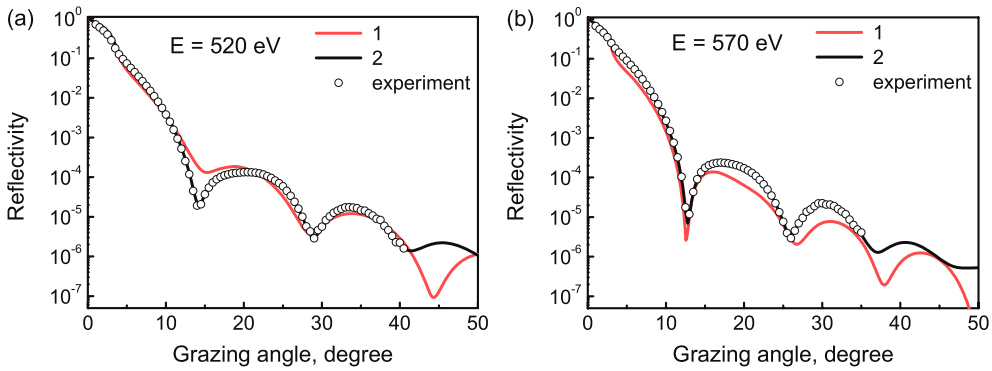

Figure 7. The measured reflectivity curves (circles) versus grazing angle at two energies ((a) 520 and (b) 570 eV) of the 5 nm thick HfO_2 film deposited onto a Si substrate by the MOCVD technique. Curves 1 and 2 are the result of fitting with the use of the single-layer (1) or three-layer (2) models.

phase of a reflected wave. An approach to the exact solution of the phase problem was developed in [15] and applied to a growing layered structure, whose reflectivity is measured *in situ* so that the reflectivity $R(t)$ and its derivative $\mathrm{d}R/\mathrm{d}t$ are known at a certain time t. These two values are sufficient to determine uniquely the phase of the reflectivity amplitude at time t.

Finally, none of the samples can be considered to be perfectly smooth for short wavelength soft x-ray radiation. Evidently, the effect of surface and interfacial roughness, which increases with increasing grazing angle, results in a deformation of the reflectivity curve and, hence, in an additional error in a reconstructed dielectric constant profile [14]. Hence, a correct solution of the inverse problem implies the measurement of x-ray scattering diagrams in parallel to reflectivity measurements to deduce roughness parameters and to take roughness effects into account during the reconstruction of the dielectric constant profile [16]. However, neither *in situ* reflectivity of a growing film, nor *ex situ* reflectivity and scattering patterns in the hard x-ray region, were measured in the first steps of our experiments. Therefore, in the present paper the analysis of reflectivity curves is restricted to the use of simple models for the samples studied.

The simplest model is a uniform HfO_2 film on a uniform Si substrate. The four fitting parameters are density and thickness of the film as well as the rms roughness σ of film interfaces, the effect of roughness being taken into account by introducing Nevot–Croce factor to the amplitude reflectivity of each interface [17]:

$$r(\theta) = r_0(\theta)\exp\left[-\frac{1}{2}\left(\frac{4\pi\sigma}{\lambda}\right)^2\sqrt{\varepsilon_\mathrm{A}-\cos^2\theta}\sqrt{\varepsilon_\mathrm{B}-\cos^2\theta}\right] \quad (3)$$

where r and r_0 are the amplitude reflectivities of a rough and a perfectly smooth interface between materials with the dielectric constants ε_A and ε_B, and θ is the grazing angle of an incident beam.

The accuracy of the fitting procedure is demonstrated in figures 6 and 7, curves 1. Both reflectivity curves of each sample were processed simultaneously. As can be seen, the simplest model describes adequately the measured reflectivities of the ALD film, while this is not the case for the MOCVD film.

A more sophisticated model implies that the samples contain three layers, namely, a HfO_2 film, a silicon surface oxide layer on a Si substrate, and an adhesion layer glued to a HfO_2 film surface and consisting mainly of molecules

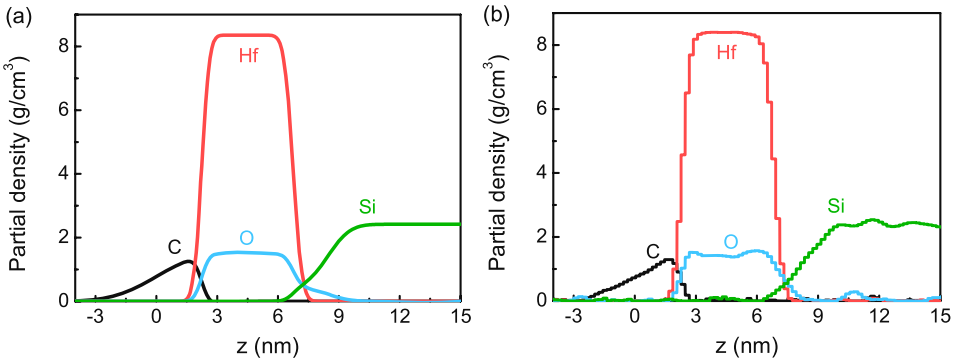

Figure 8. Depth distribution of chemical elements for the 5 nm thick HfO_2 film deposited onto a Si substrate by the ALD technique. (a) Three-layer model. (b) Result of a numerical refinement.

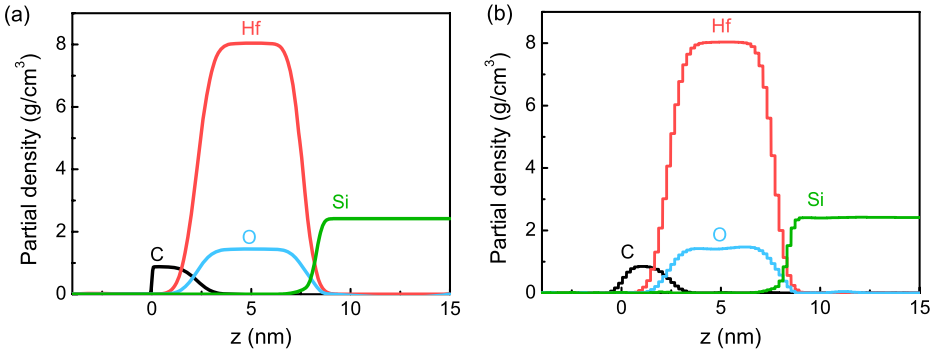

Figure 9. Depth distribution of chemical elements for the 5 nm thick HfO_2 film deposited onto a Si substrate by the MOCVD technique. (a) Three-layer model. (b) Result of a numerical refinement.

of hydrocarbons, water, and oxygen. For simplicity it will be assumed below that the adhesion layer consists of carbon molecules only. The number of fitting parameters is then 10 in the context of this model. The accuracy of the fitting procedure is demonstrated by figures 6 and 7, curves 2. It is interesting that the three-layer model describes very well the reflectivities of the MOCDV sample, while the accuracy of fitting is not essentially changed for the ALD sample when compared to the single-layer model. Evidently, if the experimental error is negligible, a small difference between the calculated and the measured reflectivity of the ALD sample observed at grazing angles exceeding 30° is connected with a simplification of the model used. Actually, the following procedure can be used to refine the model.

First of all, we note that the angular width of the detector entrance aperture was about 2° in our experiments. This means that the radiation scattered by the long-scale conformal roughness with a large correlation length was detected when measuring the reflectivity. Hence, the short-scale roughness of different interfaces, which are typically nonconformal (see, e.g., [18]), affects only the experimental reflectivity. The effect of short-scale nonconformal roughness on the reflectivity can be described in two equivalent manners: first, introducing the Nevot–Croce factor to the reflectance amplitude of each interface, as we did above, and, second, introducing a smooth variation of the dielectric constant at each interface.

If the roughness height is distributed in accordance with the normal law, an 'effective' transition layer formed near a rough interface as a result of short-scale roughness averaging is written as

$$\varepsilon(z) = \frac{\varepsilon_A + \varepsilon_B}{2} - \frac{\varepsilon_A - \varepsilon_B}{2}\mathrm{erf}\left(\frac{z}{\sigma\sqrt{2}}\right) \qquad (4)$$

where $\mathrm{erf}(x)$ is the error function. The depth distributions of chemical elements obtained by using this representation and within the framework of the three-layer model are shown in figures 8 and 9, left graphs. The Z-axis is directed into the depth of a sample. The corresponding reflectivity curves coincide with those shown in figures 6 and 7, curves 2.

Now we can refine the three-layer model. In order to do so, we represented the depth distribution of each chemical element concentration as a piecewise continuous function having a constant value within a 0.2 nm step. The total number of steps was chosen to be 100. Then we performed the fitting procedure considering the concentration of each element within one step as an unknown parameter. Notice that we used a special merit function to find a solution closest to the three-layer model. The results of fitting are shown in figures 8 and 9, right graphs. Some deviations from the three-layer model are seen. The corresponding reflectivities are shown in figure 6, curves 3, for the ALD sample, which are in a perfect agreement with the experimental data. The calculated reflectivities of the MOCVD samples are not shown in figure 7, because they cannot be distinguished from curves 2, by applying the fitting procedure. Such a situation can occur when the film is structurally inhomogeneous. It can be assumed that the

film synthesized by MOCVD is structurally inhomogeneous in depth.

The results of calculations demonstrate that the three-layer model is not inconsistent with the experimental data, but the uniqueness of the model used cannot be guaranteed. Moreover, we observe some inconsistencies between the profiles of two samples studied, e.g., between concentration profiles of silicon in a near surface layer of identical substrates used in experiment as well as between the profiles of an adhesion layer. Therefore, future experiments should include measurements and analysis of a larger set of reflectivity curves measured in a wider spectral range from hard x-rays to EUV radiation as well as of a set of scattering diagrams measured at different grazing angles of the probe beam. The latter is of extreme importance to distinguish between a real variation of chemical element concentration and the effect of short-scale roughness.

4. Summary

The microstructure of films of different thicknesses synthesized by ALD and MOCVD was characterized by reflection spectroscopy, x-ray diffraction (XRD), and soft x-ray reflectometry techniques. It was shown that near-edge reflection spectra and absorption spectra calculated on the basis of reflection spectra are very sensitive even to signatures of ordering on a subnanometer scale in the film. It was established that the microstructure of the HfO_2 film is strongly dependent on the film thickness. The study of the 5 nm thick films synthesized by ALD and MOCVD methods shows that the film prepared by ALD is amorphous. The film grown by MOCVD showed signs of crystalline structure. First results on the reconstruction of the depth distribution of chemical elements based on the analysis of reflectivity curves were discussed. The element depth profiling shows that there are no measurable differences between 5 nm ALD and MOCVD films that would provide a direct support to the importance of the structural factor. The calculations carried out allow us to assume that MOCVD film is inhomogeneous in depth. It was established that to distinguish between a real variation of the chemical element concentration and the effect of short-scale roughness, both a large set of reflectivity curves measured in a wide spectral range from the hard x-ray to EUV region and a set of scattering diagrams measured at different grazing angles of the probe beam are required.

Acknowledgments

This work was supported by the ISTC (project 3401). E Yu Taracheva gratefully acknowledges financial support from BESSY. The XRD measurements were supported by the national educational program ‘Innovative university educational program’ and the pilot project ‘Molecular geochemistry and biogeochemistry’. The authors thank Dr Stefan DeGendt (IMEC, Belgium) for providing ALD and MOCVD HfO_2 layers and Dr Fred Senf from the Optics Beamline, Centre of Synchrotron Radiation, BESSY, for help in carrying out the experiment.

References

[1] Kukli K, Aarik J, Aidla A, Simon H, Ritala M and Leskela M 1997 *Appl. Surf. Sci.* **112** 236
[2] Hsu C T, Su Y K and Yokoyama M 1992 *Japan. J. Appl. Phys.* **31** 2501
[3] Sayan S *et al* 2005 *Int. Conf. on Characterization and Metrology for ULSI Technology (Dallas)* pp 92–101
[4] Ceresoli D and Vanderbilt D 2006 *Phys. Rev.* B **74** 125108
[5] Lucovsky G *et al* 2007 Power Point Presentation www.isde.vanderbilt.edu/content/muri2007/lucovsky
[6] McComb D W 1996 *Phys. Rev.* B **54** 7094
[7] Kremmer S, Wurmbauer H, Teichert C, Tallarida G, Spiga S, Wiemer C and Fanciulli M 2005 *J. Appl. Phys.* **97** 074315
[8] Filatova E, Lukyanov V, Barchewitz R, André J-M, Idirk M and Stemmler Ph 1999 *J. Phys.: Condens. Matter* **11** 3355
[9] Stemmer S, Chen Z Q, Zhu W J and Ma T P 2003 *J. Microsc.* **210** 74
[10] Lucovsky G, Hong J G, Fulton C, Zou Y, Nemanich R J and Ade H 2004 *J. Vac. Sci. Technol.* B **22** 2132
[11] Rusakov A A 1977 *The X-Ray Diffraction of Metals* (Moscow: Atomizdat) in Russian
[12] Zhou X-L and Chen S-H 1995 *Phys. Rep.* **257** 223–348
[13] Tolan M 1999 *X-Ray Scattering from Soft-Matter Thin Films* (*Springer Tracts in Modern Physics* vol 148) (Berlin: Springer)
[14] Kozhevnikov I V 2003 *Nucl. Instrum. Methods* A **508** 519–41
[15] Kozhevnikov I V, Peverini L and Ziegler E 2008 *Opt. Express* **16** 144–9
[16] Ziegler E, Kozhevnikov I and Peverini L 2008 *Proc. 9th Int. Conf. on the Physics of X-Ray Multilayer Structure*
[17] Nevot L and Croce P 1980 *Rev. Phys. Appl.* **15** 761
[18] Peverini L, Ziegler E, Bigault T and Kozhevnikov I 2005 *Phys. Rev.* B **72** 045445